Analytic S-Shaped Temperature Dependence of Peak Positions of the Localized-State Ensemble Luminescence and Application in the Analysis of Luminescence in Non- and Semi-Polar InGaN/GaN Quantum-Wells Micro-Array

Xiaorui Wang(王晓瑞)[1] and Shijie Xu(徐士杰)[1,2*]

[1]*Department of Physics, and Shenzhen Institute of Research and Innovation (HKU-SIRI), The University of Hong Kong, Pokfulam Road, Hong Kong, China*
[2]*Department of Optical Science and Engineering, School of Information Science and Technology, Fudan University, Shanghai 200438, China*

(Received 1 August 2022; accepted manuscript online 14 September 2022)

Two analytic expressions of temperature-dependent peak positions employing the localized-state ensemble (LSE) luminescence model are deduced for the cases of $\Delta E = E_a - E_0 > 0$ and < 0, respectively, under the first-order approximation of Taylor's expansion. Then, the deduced formulas are applied to examine the experimental variable-temperature photoluminescence data of non- and semi-polar InGaN/GaN quantum-wells (QWs) array by jointly considering the monotonic bandgap shrinking described by Pässler's empirical formula. S-shaped temperature dependence of luminescence peaks of both non- and semi-polar QWs is well reproduced with the analytic formulas. As a result, the localization depths are found to be 31.5 and 32.2 meV, respectively, for non- and semi-polar QWs.

DOI: 10.1088/0256-307X/39/10/107801

Luminescence or light emission is a fundamental natural and physical phenomenon and works as the basis of laser didoes and light emitting didoes.[1–4] Therefore, gaining a better understanding of luminescence mechanisms is highly desirable for improving efficiency of light emitting devices and other optoelectronic devices. Variable-temperature photoluminescence (PL) spectroscopy is an important methodology for studying materials' luminescence mechanisms[5–7] and carrier dynamics.[8] For example, variable-temperature PL is frequently used to investigate temperature dependence of the fundamental bandgap of semiconductors, which usually monotonically shrinks with increasing the temperature.[9–12] Such shrinking behavior may be induced by both lattice dilatation and electron-phonon interactions,[13] which is described by several empirical formulas, such as Varshni's,[13] Pässler's,[14] and Bose–Einstein model formula.[15] However, in many cases of semiconductor alloys, such as $In_xGa_{1-x}N$[16,17] and $Al_xGa_{1-x}N$,[18,19] temperature dependence of luminescence peak positions is found to often show a non-monotonic redshift-blueshift-redshift evolution (usually called S-shaped dependence) with temperature from cryogenic temperature to room temperature. In some cases, the blueshift may start at cryogenic temperatures.[20] To explain the blueshift, a band tail model was proposed, in which the localized carriers were suggested at the band tail position of a Gaussian distribution.[21] However, such a band tail model cannot explain the redshift of luminescent peak positions in a low temperature range. To explain the whole S-shaped temperature dependence, we have developed the so-called localized-state ensemble (LSE) luminescence model before.[22–24] Since its establishment, the LSE model has been used by different groups to interpret the experimental temperature dependence of luminescence peak position, intensity and even spectral width of many materials including InGaN alloys,[22] polar InGaN/GaN quantum wells (QWs),[25] GaSbBi/GaAs quantum dots (QDs),[26] $Zn_{1-x}Cd_xSe$/ZnSe QWs,[27] and hybrid lead halide perovskites,[28] etc. This model has also been cited by Klingshirn and Grundmann, respectively, in the modification editions of their well-known textbooks.[29,30]

It is known that the practical applications of the LSE model are based on numerically solving a nonlinear equation with exponential terms in the model. There exists some certain difficulty to numerically solve this nonlinear equation for a key dimensionless coefficient of $x(T)$. In this Letter, we attempt to find analytic expressions of this coefficient under the first-order approximation of Taylor's expansion for the two possible cases. Finally, we apply the analytic formulas to quantitatively reproduce S-shaped temperature dependence of PL peak positions in non-polar and semi-polar InGaN/GaN QWs micro-array samples.[8] Good agreement between theory and experiment is achieved so that the localization depths of 31.5 and 32.2 meV are determined for the non- and semi-polar QWs, respectively.

The LSE model begins with a rate equation proposed in Ref. [31] for describing radiative and non-radiative dynamics of localized carriers in a localized-state system:[22,23]

$$\frac{dN(E,T)}{dt} = g\rho(E) - \frac{N(E,T)}{\tau_r} - \frac{N(E,T)}{\tau_{tr}} e^{(E-E_a)/(k_B T)} + \gamma \int_{-\infty}^{\infty} \frac{N(E',T)}{\tau_{tr}} e^{(E'-E_a)/(k_B T)} dE' \times \frac{\rho(E)}{\int_{-\infty}^{\infty} \rho(E')dE'}. \quad (1)$$

Here, $N(E,T)$ is the carrier density at localized state with

*Corresponding author. Email: sjxu@hku.hk
© 2022 Chinese Physical Society and IOP Publishing Ltd

energy of E at temperature of T, and t is time. On the right side of Eq. (1), the first term represents the optically or electrically excited generation of carriers in which g is the generating coefficient. The second one describes the localized carriers' radiative recombination in which $\tau_{\rm r}$ is the radiative time constant. The third one talks about the localized carriers' thermal escaping from the localized states, in which $\tau_{\rm tr}$ is a time constant for thermal escaping of localized carriers, $E_{\rm a}$ represents a specific energy level depending on materials and optical (electrical) excitation intensities, and $k_{\rm B}$ is the Boltzmann constant. The fourth term considers the recapture of thermally escaped carriers by the localized states, in which coefficient γ stands for the recapturing coefficient of the thermally escaped carriers, and $\rho(E)$ is the density of states (DOS) of localized states. Under the steady-state conditions, i.e., $dN(E,T)/dt = 0$, a solution to Eq. (1) may be found as follows:[23]

$$N(E,T) = g\tau_{\rm tr}\Big\{1-\gamma\Big[\int_{-\infty}^{\infty} n(E',T)e^{(E'-E_{\rm a})/(k_{\rm B}T)}dE'\Big] \cdot \Big[\int_{-\infty}^{\infty}\rho(E')dE'\Big]^{-1}\Big\}^{-1} n(E,T), \tag{2}$$

$$n(E,T) = \frac{1}{e^{(E-E_{\rm a})/(k_{\rm B}T)}+\tau_{\rm tr}/\tau_{\rm r}}\rho(E). \tag{3}$$

Herein, $n(E,T)$ can be viewed as a product of Fermi–Dirac-like distribution function and DOS of localized states, and it basically describes the line shape of localized-state ensemble luminescence.[23] Considering a Gaussian-type DOS of localized-state ensemble as $\rho(E) = \rho_0\exp(-(E-E_0)^2/(2\sigma^2))$, with E_0 and σ representing the central energy and the width of Gaussian distribution, respectively, one can find the peak position of $n(E,T)$ through solving the equation obtained by setting $\partial n(E,T)/\partial E = 0$:[22,23]

$$E = E_0 - xk_{\rm B}T, \tag{4}$$

where x is a dimensionless coefficient that can be obtained by solving the following nonlinear equation:[22,23]

$$xe^x = \Big[\Big(\frac{\sigma}{k_{\rm B}T}\Big)^2 - x\Big]\cdot\frac{\tau_{\rm r}}{\tau_{\rm tr}}e^{(E_0-E_{\rm a})/k_{\rm B}T}. \tag{5}$$

It physically means $(E_0-E)/k_{\rm B}T$, which is a function of temperature.

Equations (4) and (5), combined with the thermal shrinking of the bandgap described by Varshni's or Pässler's empirical formula, have been used by different groups to quantitatively explain the S-shaped luminescence peak position shift in different materials.[22–24,32–34]

As pointed out by Li *et al.*[23,24] and proven in practical applications, the energy difference of $\Delta E = E_{\rm a} - E_0$ plays an important role in determining the details of S-shaped temperature dependence of luminescence peak. This energy difference may be viewed as the well-noted thermal activation energy. It has been identified that ΔE can take either a positive or negative value, depending on materials and details of localized-state systems under certain excitation conditions. For instance, negative values of ΔE may be adopted to explain the S-shaped temperature dependence of PL peaks in usual polar InGaN/GaN QW samples.[24,35] In practical applications of the LSE model, it is found that there exists some difficulty to find out solution to Eq. (5), which is a complicated nonlinear equation containing exponential terms. In the following, we show that two approximate analytic solutions to Eq. (5) can be obtained for positive and negative values of ΔE, respectively.

When the temperature is approaching zero, line shape of luminescence spectrum of an LSE system described by Eq. (3) may be written as

$$n(E,T\to 0) = \begin{cases}\frac{\tau_{\rm r}}{\tau_{\rm tr}}\rho_0 e^{-(E-E_0)^2/(2\sigma^2)}, & E < E_{\rm a},\\ 0, & E > E_{\rm a}.\end{cases} \tag{6}$$

For the case of $E_{\rm a} > E_0$ or $\Delta E > 0$, the luminescence peak position is located at E_0 at 0 K. At a temperature higher than 0 K, x shall take a small value close to $(E_0-E)/k_{\rm B}T$. Using the first-order Taylor approximation, i.e., $e^x \approx (1+x)$, we can find out an approximate analytical solution to Eq. (5):

$$x \approx x_{\rm P} = \sqrt{\frac{1}{4}(\xi+1)^2 + \Big(\frac{\sigma}{k_{\rm B}T}\Big)^2\xi} - \frac{1}{2}(\xi+1), \tag{7a}$$

$$\xi = \frac{\tau_{\rm r}}{\tau_{\rm tr}}e^{(E_0-E_{\rm a})/(k_{\rm B}T)}. \tag{7b}$$

Therefore, Eq. (4) may be approximated as

$$E = E_0 - x_{\rm P}k_{\rm B}T \quad \text{for} \quad \Delta E > 0. \tag{8}$$

Taking the bandgap shrinking into consideration, temperature dependence of the luminescent peak position of localized-state ensemble may be expressed as

$$E = E_0 - \frac{\alpha\Theta}{2}\Big[\sqrt[P]{1+\Big(\frac{2T}{\Theta}\Big)^P} - 1\Big] - x_{\rm P}k_{\rm B}T \quad \text{for} \quad \Delta E > 0, \tag{9}$$

where α, Θ, and P are the Pässler's parameters.

For the case of $E_{\rm a} < E_0$ or $\Delta E < 0$, as the temperature is approaching 0 K, the luminescence peak position shall approach $E_{\rm a}$ according to Eq. (6). Letting $x = \frac{E_0-E_{\rm a}-y}{k_{\rm B}T}$ and putting it into Eq. (5), we can reach

$$\frac{E_0-E_{\rm a}-y}{k_{\rm B}T} = \Big[\Big(\frac{\sigma}{k_{\rm B}T}\Big)^2 - \frac{E_0-E_{\rm a}-y}{k_{\rm B}T}\Big]\frac{\tau_{\rm r}}{\tau_{\rm tr}}e^{\frac{y}{k_{\rm B}T}}. \tag{10}$$

Since $y = E - E_{\rm a}$ is utilized in the above transformation, it usually takes a very small value even though at a temperature higher than 0 K. With the first-order Taylor approximation of $e^{\frac{y}{k_{\rm B}T}} \approx (1+\frac{y}{k_{\rm B}T})$, an analytical solution to Eq. (10) could be obtained as follows:

$$y \approx \Big[\frac{-A+\sqrt{A^2-4B\tau_{\rm r}/\tau_{\rm tr}}}{2\tau_{\rm r}/\tau_{\rm tr}}\Big]k_{\rm B}T, \tag{11a}$$

where

$$A = \frac{\tau_{\rm r}}{\tau_{\rm tr}}\Big[\Big(\frac{\sigma}{k_{\rm B}T}\Big)^2 - \frac{E_0-E_{\rm a}}{k_{\rm B}T} + 1\Big] + 1, \tag{11b}$$

$$B = \frac{\tau_{\rm r}}{\tau_{\rm tr}}\Big[\Big(\frac{\sigma}{k_{\rm B}T}\Big)^2 - \frac{E_0-E_{\rm a}}{k_{\rm B}T}\Big] - \frac{E_0-E_{\rm a}}{k_{\rm B}T}. \tag{11c}$$

Then x is approximately expressed as

$$x \approx x_N = \frac{E_0-E_{\rm a}}{k_{\rm B}T} - \frac{-A+\sqrt{A^2-4B\tau_{\rm r}/\tau_{\rm tr}}}{2\tau_{\rm r}/\tau_{\rm tr}}. \tag{12}$$

Thus, another approximate expression of Eq. (4) would be written as

$$E = E_0 - x_N k_B T \quad \text{for} \quad \Delta E < 0. \tag{13}$$

Taking the bandgap shrinking (i.e., the Pässler's empirical formula) into consideration, one may obtain another expression of temperature-dependent luminescence peak position as

$$E = E_0 - \frac{\alpha\Theta}{2}\left[\sqrt[P]{1+\left(\frac{2T}{\Theta}\right)^P} - 1\right] - x_N k_B T \quad \text{for } \Delta E < 0. \tag{14}$$

In the following, we present an application example of the analytical expressions of temperature-dependent peak positions employing the LSE luminescence model. The variable-temperature PL spectral experiments were carried out on a strain-relaxed non- and semi-polar InGaN/GaN QWs micro-array which was overgrown on etched GaN substrate on r-plane sapphire by Wang's group with metalorganic vapor-phase epitaxy (MOVPE) technique.[36] Figure 1 shows a schematic diagram of the studied sample containing three periods of non- and semi-polar QWs. In the sample, three periods of InGaN/GaN QWs were overgrown on the etched GaN substrate with the patterned pyramid-shaped micro-holes. The top plane was the non-polar facet ($11\bar{2}0$), whereas the exposed multiple side facets were various semi-polar facets. The details of such GaN patterned substrate and overgrowth of multiple QWs have been described before.[37]

Variable-temperature PL spectra of the sample were measured on a home-assembled PL system with high spectral resolution.[38] During the PL measurements, the sample was closely attached on the cold finger of a Janis closed-cycle cryostat with a temperature varying range from 4.15 to 300 K. A 325 nm He-Cd laser (IK3401R-F, Kimmon Co. Ltd) with maximum output power of 40 mW was employed as the optical excitation source. The PL signal was collected and guided by a pair of convex lenses into the entrance slide of a monochromator (SPEX 750M) and detected by a thermoelectrically cooled photomultiplier (Hamamatsu R928). In addition, standard lock-in amplifier (SR850, Stanford Research) was employed to enhance the signal-to-noise ratio in the variable-temperature PL measurements.

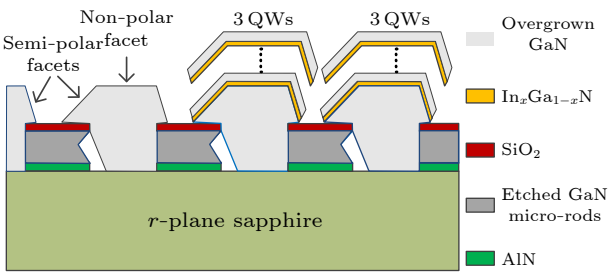

Fig. 1. Schematic diagram (not in scale) of non- and semi-polar InGaN/GaN QWs micro-array.

Figure 2(a) shows excitation-power-dependent PL spectra (in semi-logarithmic scale) of the sample measured at 4.15 K. The PL peaks labeled as P1 and P2 correspond to the PL signals from non-polar ($11\bar{2}0$) and semi-polar ($10\bar{1}\bar{1}/01\bar{1}\bar{1}$) QWs.[8,36] At high energy side of P1, two PL peaks at 3.417 and 3.474 eV may originate from the radiative recombination of basal-plane stacking-fault related exciton and free exciton in GaN layers, respectively.[8] As is shown and marked by dashed vertical lines in Fig. 2(a), with the excitation power increasing from 0.17 to 21.2 mW, various PL peak positions keep unchanged, indicating the strain relaxed property of the studied sample. In contrast, PL peak positions of strained polar InGaN/GaN QW samples usually show substantial blueshifts with the increasing excitation power, caused by the screening effect of photogenerated carriers on the QW transitions (or called reverse quantum confinement Stark effect).[24,39]

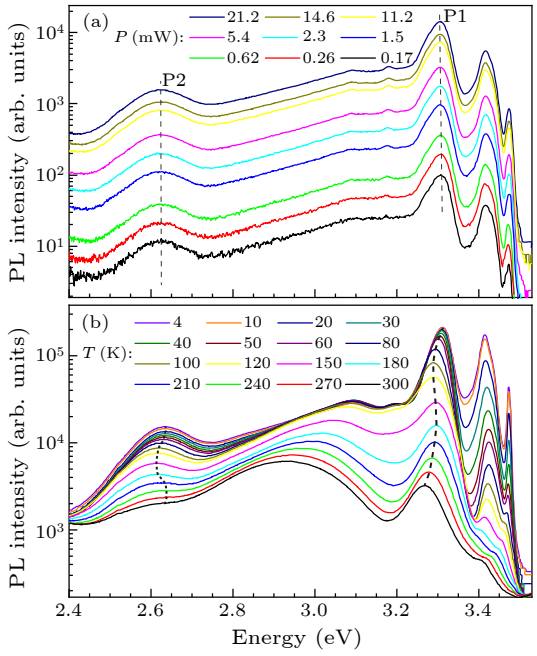

Fig. 2. Excitation-power and temperature-dependent PL spectra (in semi-logarithmic scale) of the studied QW sample. (a) Excitation-power dependent PL spectra measured at 4.15 K. (b) Temperature-dependent PL spectra measured at a fixed excitation power of 21.2 mW. Two dotted lines are of guide to the eyes.

Figure 2(b) shows temperature-dependent PL spectra (also in semi-logarithmic scale) of the QW sample. Both PL peaks of the non- and semi-polar QWs exhibit typical S-shaped temperature dependence of LSE luminescence. For instance, the peak position of P1 redshifts from 3.314 eV at 4.15 K to 3.292 eV at 100 K, then blueshifts to 3.300 eV at 180 K, and finally re-redshifts to 3.270 eV at 300 K. The peak position of P2 also displays similar temperature dependence. In contrast to both P1 and P2, the free-exciton PL peak in GaN layers shows a normal continuous redshift behavior from cryogenic to room temperature. Figures 3(a), 3(b) and 3(c) show the peak positions (solid symbols) of the free-exciton transition, P1 and P2, respectively.

The solid line in Fig. 3(a) represents a fitting curve with the Pässler's empirical formula:

$$E = E_0 - \frac{\alpha\Theta}{2}\left[\sqrt[P]{1+\left(\frac{2T}{\Theta}\right)^P} - 1\right]. \tag{15}$$

The fitting parameters are tabulated in Table 1. The hori-

zontal dotted line marks the location of E_0 for the free exciton luminescence of GaN layer. Good agreement between experiment and the model is achieved for the free-exciton luminescence peak in the studied QW sample. This means that the monotonic redshift of the GaN free-exciton luminescence peak distinctly follows the GaN bandgap shrinking with increasing the temperature. However, the PL peaks of the strain relaxed non- and semi-polar QWs show typical S-shaped temperature dependence due to the carrier localization caused by local In enriching clusters or phase separation. For both non- and semi-polar QWs studied in the present work, $E_a > E_0$ or $\Delta E > 0$ may be satisfactory because of the absence of huge piezoelectric fields in the sample. We thus employ Eq. (9) to analyze the temperature dependence of both PL peaks. In Figs. 3(b) and 3(c), the solid lines depict fitting curves with Eq. (9) for the experimental PL peak positions (solid squares) of P1 and P2, respectively. In the figures, the respective temperature dependence of LSE luminescence peak and bandgap shrinking are also drawn in different color curves for P1 and P2. In addition, the energetic locations of E_a and E_0 are also marked with horizontal dashed and dotted lines as references, respectively. Fitting parameters of P1 and P2 are summarized in Table 1. The localization depths of ΔE are found to be 31.5 meV and 32.2 meV for the non- and semi-polar QWs, respectively. The values of fitting parameters including the width of Gaussian distribution are obtained through fitting the experimental data of temperature-dependent PL peak positions via using the least squares method.

From the fitting results in Fig. 3, one may have these concluding remarks: (1) The temperature dependence of the free exciton luminescence peak of GaN layers follows a simple monotonic bandgap shrinking with temperature in the interested temperature range from cryogenic to room temperature because of large binding energy (∼25.4 meV) of the free excitons in GaN.[40] (2) For the localized-state luminescence in both non- and semi-polar QWs, the redshift and the following blueshift of the PL peak positions in low and medium high temperature ranges are mainly caused by the thermal escaping and re-distribution of localized carriers, respectively. (3) At higher temperatures, once again redshift of the PL peak positions is dominated by the bandgap shrinking.

It is worth noting that analytic expression of the LSE luminescence peak position under the conditions of $\Delta E = E_a - E_0 < 0$, i.e., Eq. (14), can be used to well interpret the experimental S-shaped temperature dependence of PL peak position in different materials, i.e., the strained polar InGaN/GaN QWs.[35] However, in these cases, a negative thermal activation energy, i.e., $\Delta E < 0$, may occur. Although the S-shaped curve is also well reproduced with Eq. (14), the initial luminescence peak of the LSE states with $E_a < E_0$ is near E_a at $T \to 0$ K rather than at E_0 in the cases of $E_a > E_0$.

Finally, we would like to point out that the size effect may become significant in ultra-small size micro-LEDs as investigated by Yu *et al.* in a latest study.[41] As the micro-LED feature size approaches the carrier diffusion length, the size effect may have a strong influence on luminescence property of QWs, which needs to be further investigated.

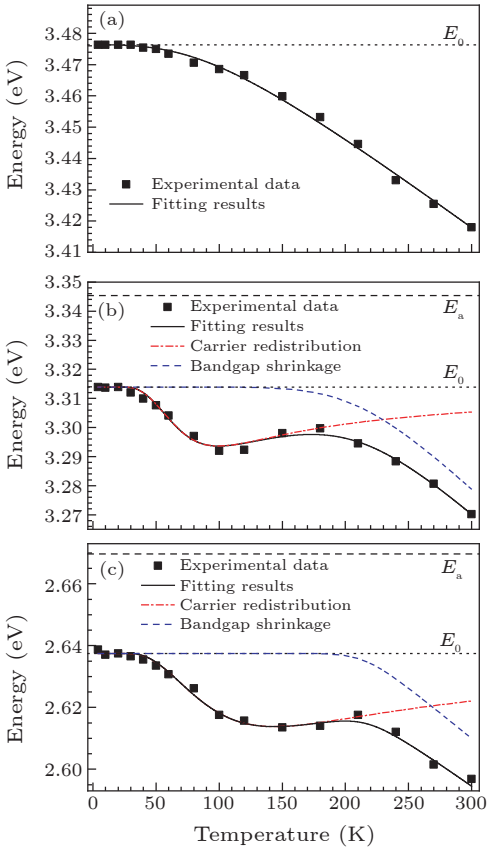

Fig. 3. Experimental PL peak positions (solid squares) of GaN free-exciton (a), non- (b) and semi-polar QWs (c). Their corresponding fitting curves are drawn in solid lines. In addition, the LSE fitting curves and the bandgap shrinking curves described by the Pässler's empirical formula are given.

Table 1. Fitting parameters of different PL peaks.

Peak	E_0 (eV)	ΔE (meV)	σ (meV)	τ_r/τ_{tr}	α (10^{-4} eV/K)	Θ (K)	P
GaN exciton	3.476				2.99	220	2.9
Non-polar QW	3.314	31.5	15	452	4.1	434	7.9
Semi-polar QW	2.638	32.2	20.6	88	3.3	433	19

In summary, approximate analytic solutions of temperature-dependent peak positions by employing the LSE luminescence model are deduced for the cases with positive ($\Delta E > 0$) and negative ($\Delta E < 0$) thermal activation energies, respectively. It is validated that S-shaped temperature dependence of PL peak position can be interpreted in both cases when the monotonic shrinking of bandgap is also taken into account. The experimental data of variable-temperature luminescence in a strain-relaxed non-polar and semi-polar InGaN/GaN QWs micro-array are well fitted by the analytic expression of the LSE model with positive thermal activation energy ($\Delta E > 0$). Lo-

calization depths of 31.5 meV and 32.2 meV are found for the non- and semi-polar QWs, respectively, via the fitting. The analytic solution by the LSE model with $\Delta E < 0$ can also be employed to fit the S-shaped temperature dependence of PL peak position, i.e., for strained polar InGaN/GaN QWs. However, there exists some distinct difference between the two cases of $\Delta E > 0$ and $\Delta E < 0$. The derivation of analytic expressions of S-shaped temperature-dependent peak position of LSE model may further boost practical applications of LSE model in the quantitative understanding of localized-state luminescence in different materials.

Acknowledgments. This work was supported by the National Natural Science Foundation of China (Grant No. 12074324), and Science, Technology, and Innovation Commission of Shenzhen Municipality (Grant No. JCJY20180508163404043). One of the authors, SJX, would be grateful to Professor T. Wang for providing high-quality samples of InGaN/GaN QWs micro-array.

References

[1] Yoshida H, Yamashita Y, Kuwabara M, and Kan H 2008 *Nat. Photon.* **2** 551
[2] Schneider C, Rahimi-Iman A, Kim N Y, Fischer J, Savenko I G, Amthor M, Lermer M, Wolf A, Worschech L, Kulakovskii V D, and Shelykh I A 2013 *Nature* **497** 348
[3] Funato M, Kaneta A, Kawakami Y, Enya Y, Nishizuka K, Ueno M, and Nakamura T 2010 *Appl. Phys. Express* **3** 021002
[4] Wang T, Liu Y H, Lee Y B, Ao J P, Bai J, and Sakai S 2002 *Appl. Phys. Lett.* **81** 2508
[5] Zelewski S J, Urban J M, Surrente A, Maude D K, Kuc A, Schade L, Johnson R D, Dollmann M, Nayak P K, Snaith H J, and Radaelli P 2019 *J. Mater. Chem. C* **7** 8350
[6] Cheche T O, Chang M C, and Lin S H 2005 *Chem. Phys.* **309** 109
[7] Shi S L, Li G Q, Xu S J, Zhao Y, and Chen G H 2006 *J. Phys. Chem. B* **110** 10475
[8] Wang X, Wang T, Yu D, and Xu S 2021 *J. Appl. Phys.* **130** 205704
[9] Tiginyanu I M, Ursaki V V, Zalamai V V, Langa S, Hubbard S, Pavlidis D, and Föll H 2003 *Appl. Phys. Lett.* **83** 1551
[10] Reshchikov M A, Huang D, Yun F, Visconti P, He L, Morkoç H, Jasinski J, Liliental-Weber Z, Molnar R J, Park S S, and Lee K Y 2003 *J. Appl. Phys.* **94** 5623
[11] Wang K, Araki T, Yamaguchi T, Chen Y T, Yoon E, and Nanishi Y 2015 *J. Cryst. Growth* **430** 93
[12] Zhang X T, Liu Y C, Zhi Z Z, Zhang J Y, Lu Y M, Shen D Z, Xu W, Fan X W, and Kong X G 2002 *J. Lumin.* **99** 149
[13] Varshni Y P 1967 *Physica* **34** 149
[14] Pässler R 1996 *Phys. Status Solidi B* **193** 135
[15] Vina L, Logothetidis S, and Cardona M 1984 *Phys. Rev. B* **30** 1979
[16] Chowdhury A M, Roul B, Singh D K, Pant R, Nanda K K, and Krupanidhi S B 2020 *ACS Appl. Nano Mater.* **3** 8453
[17] Wang J, Dasari K, Cooper K, Thota V R, Wright J, Palai R, Ingram D C, Stinaff E A, Kaya S, and Jadwisienczak W M 2015 *Phys. Status Solidi C* **12** 413
[18] Kuokstis E, Sun W H, Shatalov M, Yang J W, and Asif K M 2006 *Appl. Phys. Lett.* **88** 261905
[19] Cho Y H, Gainer G H, Lam J B, Song J J, Yang W, and Jhe W 2000 *Phys. Rev. B* **61** 7203
[20] Murotani H, Yamada Y, Taguchi T, Ishibashi A, Kawaguchi Y, and Yokogawa T 2008 *J. Appl. Phys.* **104** 053514
[21] Eliseev P G, Perlin P, Lee J, and Osiński M 1997 *Appl. Phys. Lett.* **71** 569
[22] Li Q, Xu S J, Cheng W C, Xie M H, Tong S Y, Che C M, and Yang H 2001 *Appl. Phys. Lett.* **79** 1810
[23] Li Q, Xu S J, Xie M H, and Tong S Y 2005 *Europhys. Lett.* **71** 994
[24] Li Q, Xu S J, Xie M H, and Tong S Y 2005 *J. Phys.: Condens. Matter* **17** 4853
[25] Arteev D S, Sakharov A V, Zavarin E E, Lundin W V, Rzheutski M V, Lutsenko E V, and Tsatsulnikov A F 2021 *Semicond. Sci. Technol.* **36** 125007
[26] Hidouri T, Mal I, Samajdar D P, Saidi F, and Das T D 2019 *Superlattices Microstruct.* **129** 252
[27] Klochikhin A, Reznitsky A, Don Dal B, Priller H, Kalt H, Klingshirn C, Permogorov S, and Ivanov S 2004 *Phys. Rev. B* **69** 085308
[28] Wright A D, Milot R L, Eperon G E, Snaith H J, Johnston M B, and Herz L M 2017 *Adv. Funct. Mater.* **27** 1700860
[29] Klingshirn C F 2007 Semiconductor Optics Third Edition (Springer-Verlag Berlin Heidelberg) p. 366
[30] Grundmann M 2010 *The Physics of Semiconductors* 2nd edn (Berlin: Springer-Verlag) p 431
[31] Xu Z Y, Lu Z D, Yuan Z L, Yang X P, Zheng B Z, Xu J Z, Ge W K, Wang Y, Wang J, and Chang L L 1998 *Superlattices Microstruct.* **23** 381
[32] Hidouri T, Saidi F, Maaref H, Rodriguez P, and Auvray L 2016 *Opt. Mater.* **62** 267
[33] Ezzedini M, Hidouri T, M A H H, Sayari A, Shalaan E, Chauvin N, Sfaxi L, Saidi F, Al-Ghamdi A, Bru-Chevallier C, and Maaref H 2017 *Nanoscale Res. Lett.* **12** 450
[34] Arbia M B, Smiri B, Demir I, Saidi F, Altuntas I, Hassen F, and Maaref H 2022 *Mater. Sci. Semicond. Process.* **140** 106411
[35] Bao W, Su Z, Zheng C, Ning J, and Xu S 2016 *Sci. Rep.* **6** 34545
[36] Gong Y, Jiu L, Bruckbauer J, Bai J, Martin R W, and Wang T 2019 *Sci. Rep.* **9** 986
[37] Jiu L, Gong Y, and Wang T 2018 *Sci. Rep.* **8** 9898
[38] Xu S J, Li G Q, Xiong S J, and Che C M 2006 *J. Appl. Phys.* **99** 073508
[39] Li Q, Xu S J, Xie M H, Tong S Y, Zhang X H, Liu W, and Chua S J 2002 *Jpn. J. Appl. Phys.* **41** L1093
[40] Xu S J, Liu W, and Li M F 2002 *Appl. Phys. Lett.* **81** 2959
[41] Yu L M, Lu B Y, Yu P, Wang Y, Ding G J, Feng Q, Jiang Y, Chen H, Huang K, Hao Z B, Yu J D, Luo Y, Sun C Z, Xiong B, Han Y J, Wang J, Li H T, and Wang L 2022 *Appl. Phys. Lett.* **121** 042106